

The Characteristics and Influence of Biomass Burning Aerosols on Fine Particle Ionic Composition Measured in Asian Outflow During TRACE-P

Y. Ma¹, R. J. Weber¹, Y.-N. Lee², D. C. Thornton³, A. R. Bandy³, A. D. Clarke⁴, D.
R. Blake⁵, G. W. Sachse⁶, H. E. Fuelberg⁷, C. M. Kiley⁷, J.-H. Woo⁸, D. G. Streets⁹,
G. R. Carmichael⁸, F. L. Eisele¹⁰

¹School of Earth and Atmospheric Sciences, Georgia Institute of Technology, GA

²Environmental Sciences Department, Brookhaven National Laboratory, NY

³Department of Chemistry, Drexel University, Philadelphia, PA

⁴Department of Oceanography, University of Hawaii at Manoa, HI

⁵Department of Chemistry, University of California Irvine, CA

⁶NASA Langley Research Center, Hampton, VA

⁷Department of Meteorology, Florida State University, FL

⁸CGRER, University of Iowa, IA

⁹Argonne National Laboratory, IL

¹⁰Georgia Institute of Technology and National Center for Atmospheric Research

ABSTRACT

This paper investigates the role of biomass burning emissions on fine particles measured over the western Pacific Ocean during late February to early April 2001, as part of the NASA Transport and Chemical Evolution over Pacific (TRACE-P) Experiment. Airborne measurements from the NASA P3-B of fine particle ionic composition, absorbing particles, and various gaseous species are reported. Based on fine particle potassium (K^+) as a biomass tracer, approximately 10% of the TRACE-P measurements of Asian outflows were influenced by some form of biomass emissions. Relatively pure biomass burning plumes were encountered at low latitudes above the marine boundary layer (~ 3 km asl) and were found to have enhanced concentrations of fine particle potassium, ammonium, and nitrate, along with absorbing aerosols, and CO. Mixed biomass/pollution plumes were encountered at higher latitudes near the ocean surface. Based on comparisons with ratios of gas species, the ratio of fine particle potassium to sulfate (dK^+/dSO_4^{2-}) is used to provide an estimate of the relative contributions of biomass and fossil fuel combustion to fine particle mass in mixed Asian plumes. This ratio suggests that on average, approximately 30% of the aerosol mass in the mixed TRACE-P plumes is due to biomass or biofuel combustion. The characteristics of three plumes with fine particle composition that spans the range from relatively pure biomass to mainly fossil fuel emissions, are presented in detail as case studies.

INTRODUCTION

During February through April 2001, the NASA Global Tropospheric Experiment (GTE) mounted a two-aircraft (NASA Wallops P3-B and NASA Ames DC-8) airborne research campaign to investigate Asian continental outflows. The magnitude of these emissions is sufficient to influence the composition of the global atmosphere. The experiment is referred to as TRANsport and Chemical Evolution over the Pacific (TRACE-P). TRACE-P objectives include: to identify the major pathways for Asian outflow over the western Pacific, to chemically characterize the outflow, and to estimate contributions from different emission sources, such as biomass burning, and fossil fuel combustion. In this paper we focus on the contribution of biomass burning emissions to fine particle concentrations. In this case, biomass burning refers to any form of burning, including biofuel.

The chemical composition of both trace gases and aerosol particles in anthropogenic plumes provides information on emission sources. For example, the particulate potassium ion (K^+) is often a useful tracer for identifying biomass burning [Andreae, 1983; Andreae et al., 1996]. This is because the combustion of plant matter, which contains K^+ as a major electrolyte within its cytoplasm, releases large amounts of K^+ -rich particles in the submicron size fraction [Cachier et al., 1991; Gaudichet et al., 1995], and contributions of soil- or sea-spray-derived K^+ in the submicron aerosol is usually small. Various organic particulate

compounds are also uniquely found in biomass burning emissions and have been used for identifying specific sources [Schauer et al., 1996]. Elemental carbon associated with potassium has also been used as a tracer for biomass burning plumes [Andreae, 1983]. Certain trace gases are also useful tracers, including acetonitrile (CH_3CN) and carbon monoxide (CO) [Reiner et al., 2001] and methylchloride (CH_3Cl) [Blake et al., 1999]. For fossil fuel emissions, sulfur dioxide (SO_2) and tetrachloroethene (C_2Cl_4) are useful tracers.

Ambient aerosol chemical composition is typically measured by integrated filter methods. Its application to airborne plume studies through the use of tracers (biomass burning/pollution) is often restricted by the long sampling integration times and poor resolution during vertical profile flights. Here we report on higher resolution data from the Particle-Into-Liquid Sampler coupled to Ion Chromatographs (PILS-IC) for rapid and automated measurements of the aerosol particle bulk ionic composition. The aim of this paper is to investigate the fine particle ionic chemical characteristics and possible sources of biomass burning aerosols from eastern Asia, and to gauge the usefulness of particulate ionic species for estimating relative contributions of biomass versus pollution in mixed plumes.

2. EXPERIMENTAL

The TRACE-P experiment focused mainly on eastern Asia and the western Pacific Ocean. Both research aircraft, the DC-8 (ceiling 12 km) and the P-3B

(ceiling 7 km) were operated first out of Hong Kong, P. R. China (22.3°N, 113.92°E) and then the Yokota Air Force Base, Japan (35.76°N, 139.92°E) during February through April 2001. These two bases of operations were well situated to sample Asian outflow over the range of latitudes from 10°N to 50°N. The payload of the P3-B included a suite of instruments for measurements of both atmospheric gases and aerosols, and meteorological parameters. The regions investigated by the P3-B during the intensive field study were mainly within the area of 5°-45°N, 110°-155°E. The following analysis focuses only on this region. Data from the transit flights from North America to Asia and back again at the conclusion of the study are not included.

A Particle-Into-Liquid Sampler coupled to Ion Chromatographs (PILS-IC) measured fine aerosol inorganic chemical composition on the P3-B. In this instrument, sample air is first drawn through denuders to remove interfering gases and then adiabatically mixed with saturated water vapor. In this environment, sampled ambient particles grow to sizes that are easily captured by an inertial impactor. The resulting liquid flow containing the water-soluble aerosol components is then analyzed on-line and continuously with anion and cation Ion Chromatographs. The chosen analysis method permits a 4-minute duty cycle for measurement of Na^+ , NH_4^+ , Ca^{2+} , K^+ , Mg^{2+} , Cl^- , NO_3^- , and SO_4^{2-} . The PILS-IC deployed for this mission had an upper size measurement limit (50% efficiency) at 1.3 μm diameter. Limits of detection vary for specific species, but are approximately 10 ng m^{-3} (3 pptv) for the anions and 50 ng m^{-3} (45 pptv)

for cations. A more detailed instrument description is given in Weber et al. [2001] and Orsini et al. [2002]. An intercomparison of the PILS-IC to various other measurement techniques during this mission and the concurrent ACE-Asia mission is discussed elsewhere [Ma et al., 2002].

During sampling, ram air heating and heat transfer from the cabin to the sample during transport to the instrument can result in loss of semi-volatile aerosol components. For ionic components, this is most likely to result in an under-measurement of nitrate. Measurements of the difference between sample and ambient temperatures were typically about 10°K at low altitudes and about 35°K at higher altitudes making the volatility losses most severe during higher altitude measurements.

Nonmethane hydrocarbons and other trace gases were measured in whole air samples collected by the University of California-Irvine (UCI). Two liter stainless steel canisters are pressurized by a two-stage metal bellows pump and then ferried to UCI for analysis via gas chromatograph involving various techniques. The measurement precision for CH₃Cl and C₂Cl₄ was 2%. A more detailed method description is given in Sive [1998].

Concentrations of light-absorbing particles at 565 nm wavelength measured with an absorption photometer (PSAP-Radiance Research) alternatively quantified the absorption coefficient of all particles and particles smaller than 1 µm diameter. Switching an inertial impactor on or off line segregated the two size ranges. The PSAP records changes in optical

transmission through a filter onto which particles are continually collected. Filter absorption is then related to the optical absorption coefficient using Beer's law and a calibration coefficient [Bond et al., 1999]. The instrument has a detection limit better than 0.1 mg m^{-3} for 5 minutes averages.

Fast response tunable diode laser sensors measured carbon monoxide spectroscopically. The DACOM (Differential Absorption CO Measurement) instrument had a time resolution of 1 second [Sachse et al., 1991]. Sulfur dioxide was measured with an Atmospheric Pressure Ionization Mass Spectrometry (APIMS) with an average time resolution of 1 second [Thornton et al., 2002]. This technique involves a quadrupole mass spectrometer with a nickel-63 (Ni-63) source. High isotopic purity S-34 SO_2 is added to the ambient air as an internal standard.

Because the time resolution of the various measurement techniques differs, one-minute average merged data files were generated by NASA Langley Research Center and used for this analysis. The data set can be accessed through the GTE website at <http://www-gte.larc.nasa.gov>.

Five-day back-trajectories, generated by Florida State University, are also used in our analysis. The trajectories are calculated using a kinematic model employing wind components from the European Center for Medium Range Weather Forecasts (ECMWF). The dataset have 1.0-degree by 1.0-degree horizontal resolution, 61 sigma levels (terrain following coordinate system) in the vertical, and are available at 6 hour intervals throughout the TRACE-P period.

Additional details on the trajectory model, along with a comparison between kinematic and isentropic trajectories, are given in Fuelberg et al. [1996].

The University of Iowa research group provided modeling estimates of daily emissions from biomass burning for CO, Black Carbon (BC) and other species using AVHRR data provided from the World Fire Web (WFW), (<http://ptah.gvm.sai.jrc.it/wfw/>) and TOMS Aerosol Index data (<http://toms.gsfc.nasa.gov/aerosols/aerosols.html>). Emissions from biomass burning were estimated only for field combustion, which includes burning of forest, savanna, and agricultural residues. First, total emissions are estimated based on the emission database from Argonne National Laboratory (D. Streets). World Fire Web data is used for determining the spatial and temporal (daily) emissions, and TOMS-Aerosol Index (AI) is used to reduce both cloud interference and satellite coverage limitations. Emission factors for each species are then estimated by dividing the total emission by total fire count. The daily emission of each species is derived by multiplying emission factors by daily AI-adjusted fire counts.

3 RESULTS AND DISCUSSIONS

3.1 Spatial distribution and correlations

The spatial distribution of fine particulate potassium within the western Pacific region is shown in Figure 1. Peak concentrations are found at both high and low latitudes, and maximum concentrations are found between 120-130°E

longitude. The vertical K^+ profile in Figure 2 shows that concentrations are generally highest near the surface. Maximum concentrations of roughly 3000 pptv were observed in the Yellow Sea boundary layer. A peak of approximately 1000 pptv at 3 km asl was the most pure biomass plume detected in this study. Both plumes are discussed in detail in the follow sections.

To test if measured fine particle K^+ is related to biomass burning in this data set, correlations between K^+ and biomass indicators is investigated through linear regressions. Elemental Carbon (EC) is one major product of biomass burning. It is estimated that 86% of global EC emissions are from biomass burning [Andreae, 1991]. In this analysis we use measured aerosol absorption as a surrogate for EC some other absorbing aerosols, such as dust, were at low concentrations. For the data collected during all intensive TRACE-P Research Flights, K^+ is correlated with the absorption coefficient with a r^2 of 0.73, shown in Figure 3. Because higher concentrations can exert a disproportionate effect on the linear regression, a plot is also made for those K^+ concentrations less than 1000 pptv, shown in the smaller plot of Figure 3. For this data the r^2 is 0.66.

Incomplete combustion is a global source for CO, whether from wildfires or fossil fuel burning. K^+ is also correlated with CO with a r^2 of 0.61 for all research flight data, while for K^+ concentrations less than 1000 pptv, the r^2 is 0.44 (Figure 4). The positive non-near zero intercept in both the absorption (EC) and CO versus K^+ plots is likely due to background levels of EC and CO emissions

that are not directly associated with the K^+ from biomass combustion in specific plumes.

CH_3Cl is also considered a unique product of biomass burning, with 25 to 50% of CH_3Cl thought to be from biomass burning emissions [Andreae et al., 1996]. CH_3Cl concentrations are also usually not elevated in northern cities suggesting that it has no significant urban sources [Blake et al., 1997]. Although the correlation between CH_3Cl and K^+ for each plume is relatively high (r^2 ranges 0.40 - 0.72, for the three samples shown in Figure 5), differences in CH_3Cl background concentrations and the variation in K^+/CH_3Cl slopes for different plumes result in a lower than expected r^2 of 0.28, Figure 5. Differences in K^+/CH_3Cl slopes may be caused by interferences from natural production of CH_3Cl from the surface ocean water, (Singh et al., 1983) or differences in the chemical properties of K^+ and CH_3Cl . CH_3Cl is a fairly long-lived gas (approximately 1 year), while K^+ is water-soluble and readily scavenged by precipitation. Because the biomass burning influence is greater at lower latitudes in the Western Pacific, considering only data from latitudes lower than $28^\circ N$, results in a higher correlation coefficient (r^2) of 0.49. A similar result is found by comparing the $K^+ - CO$ and $CH_3Cl - CO$ correlations. The $K^+ - CO$ r^2 is 0.61 and $CH_3Cl - CO$ r^2 is 0.50.

Fine particle K^+ is also observed to be correlated with fine particle ammonium (NH_4^+) with a r^2 of 0.77 for all data and 0.51 when K^+ is lower than

1000 pptv, Figure 6. Other studies have also shown that biomass burning can be a source of NH_3 leading to fine particulate NH_4^+ (Andreae and Merlet, 2001).

Relationships between various fine particle ionic components in specific plumes also provides insights into biomass burning emissions. Although many plumes sampled in TRACE-P had measurable levels of K^+ , our detailed analysis focuses on three specific plumes.

3.2 Case studies

Three unique plumes encountered during TRACE-P are presented in more detail as case studies. These plumes were measured on three separate flights and in different locations and are identified in Figure 1. The flight 10 plume measured on March 9, 2001 2:58-3:46 UTC was apparently a relatively pure biomass plume encountered above the boundary layer. In contrast, flight 14 and 19 plumes were mixed, contained both biomass burning tracers and fossil fuel emissions. Both these plumes were located in the marine boundary layer; Flight 14 in the Yellow Sea and Flight 19 in the Sea of Japan. Flight 14 is unique in that it contained some of the highest K^+ concentrations (3000 pptv) recorded during TRACE-P, and higher than those recorded during the Pacific Exploratory Mission in the western Pacific, phase A in 1991, and B in 1994 (PEM-West A & B) where maximum concentrations were 241 pptv and 260 pptv, respectively [Dibb et al., 1997]. It is also noteworthy that these two plumes were associated with highest concentrations of newly formed 3-4 nm diameter particles observed

during TRACE-P. New particle production in these plumes is reported in Weber et al. [2002].

Case 1: Flight 10, A relatively pure biomass burning plume. The purest biomass plume recorded during TRACE P was measured north of the Philippines in the Luzon Strait. Estimates of the spatial distribution of biomass CO and black carbon emissions averaged over five days prior to the flight are shown in Figure 7. These emissions are calculated based on the method described in the Experiment section. Five-day back-trajectories and the location of the plume are also shown in the figure. Air masses at an altitude of 500hPa (~ 5.4 km asl) appear to originate from the region of Southeast Asia where over the five days prior to the plume interception experienced extensive biomass burning, most of which appears to be from Thailand. The vegetation of Southeast Asia is mainly savanna grassland and tropical forest. Surface-level back trajectories (1000hPa) in Figure 7 indicate that these air masses did not intercept the biomass burning region, but instead may have originated near Hanoi.

Aircraft altitude and fine particle ionic concentrations measured in the region of the biomass plume are shown in Figure 8. These measurements included a number of soundings and level leg runs. The sounding measurements are used to construct vertical profiles in Figure 9. Based on fine particle concentrations of K^+ and SO_4^{2-} , a temperature inversion at approximately 2.2 km asl (not plotted) appears to separate a biomass layer near 3 km asl (high

K⁺) from a surface level pollution layer (high SO₄²⁻). In both Figures 8 and 9, various aerosol species are associated preferentially in one of the two plumes, and some species are found in both. On average, the K⁺ concentration in the 3-km asl plume is 700 pptv and near zero in the surface plume. NO₃⁻ has the same trend as K⁺ and reaches its highest concentration of more than 1000 pptv, also at 3 km asl. Smaller amounts of NO₃⁻ are, however, also observed in the pollution layer. The nitrate tends to track the nitric acid measurements (shown only in Figure 9), consistent with combustion-generated NO_x leading to HNO₃ production and then particulate nitrate formation. In contrast, SO₄²⁻ shows a small increase at 3 km, possibly due to some mixing of pollution with the biomass plume, but is clearly higher at the surface. Significant amounts of sulfate are not produced from biomass burning [Chin et al., 1996]. Ammonium is found in both plumes, however highest concentrations are observed in the upper biomass plume. Although not plotted, Ca²⁺ and Na⁺ are both less than 100 pptv at 3 km asl suggesting little influence from dust or sea salt in this region.

For the ionic measurements within the biomass burning plume (altitude > 2 km asl), K⁺ is highly correlated with NO₃⁻, NH₄⁺, and SO₄²⁻, all with r² higher than 0.9. In the boundary layer pollution plume (altitude < 2 km asl), NH₄⁺ correlates with SO₄²⁻, r² = 0.80, but shows no correlation with K⁺ or NO₃⁻. The NH₄⁺/SO₄²⁻ molar ratio is also shown in Figure 9. Throughout the study it was typically near 2, as observed in the surface level pollution plume. In the biomass plume however the ratio ranges from 2 to 6. The fine particle charge balance is

also plotted. For all TRACE-P research flights, on average, positive/negative charge ratios are 0.92 (excluding data from volcanic plumes), suggesting that the PILS-IC captures most of the aerosol ionic components. The ionic balance (cations – anions, in equivalents) in figure 9 shows that about 27% of the total molar mass is missing anions necessary to achieve balance within the biomass plume. These missing anions are likely organic acids not measured, but associated with the biomass plume [Tabazadeh et al., 1998]. Although fine organic aerosol particle mass was not measured, comparisons between the sum of the PILS ionic mass and optical particle measurements of fine particle volume show that in the biomass plume the fraction of ionic mass to fine volume was significantly less than other plumes, indicating unusually large concentrations of organic species in this plume.

Case 2: Flight 14, Yellow Sea mixed biomass – pollution plume. In contrast to the more pure biomass plume, plumes containing mixtures of biomass, urban-industrial emissions, and some dust were also encountered. The most polluted plume recorded in TRACE-P was measured in the Yellow Sea during Flight 14, see Figure 1. K^+ , the fine particle absorption coefficient (likely mainly due to EC since there is little dust), CO, NH_4^+ , NO_3^- , SO_4^{2-} , and SO_2 all reach the highest concentrations of TRACE-P. Peak concentrations were 3.0 ppbv ($4.7 \mu g/sm^3$) for K^+ , 23.2 ppbv ($16.9 \mu g/sm^3$) for NH_4^+ , 15.9 ppbv ($40.2 \mu g/sm^3$) for NO_3^- , and 6.1 ppbv ($24.1 \mu g/sm^3$) for SO_4^{2-} . The total ionic mass concentration was as high as $88.9 \mu g/sm^3$. This plume was intercepted twice

during north and southbound legs. The ionic composition of the plume is shown in Figure 10. The correlation (r^2) between K^+ and SO_4^{2-} in the two passes is 0.72, suggesting strong mixing of biomass burning and fossil fuel combustion. The NH_4^+/SO_4^{2-} ratio also increases up to about 4 to 5 within the plume, but the measured ions are nearly in balance. The average of the ratio of ion balance to total ions measured (molar ratio) is less than 2%. This plume is also atypical in that NO_3^- exceeds SO_4^{2-} . NO_3^-/SO_4^{2-} molar ratios typically range between 0 and 1, however, in this plume the ratio reached 3, which is the highest of TRACE-P. Near complete ion balance between SO_4^{2-} plus NO_3^- and NH_4^+ suggests that most of it is likely NH_4NO_3 . The NO_x emission and back trajectory data suggest that the high concentration of NO_3^- may be from anthropogenic sources in the northern coastal region of China.

Based on fine particle water-soluble calcium, Figure 10 shows that there was also some influence from dust in this plume; calcium concentrations were on average 800 pptv. But relative to the total molar mass of all ions, Ca^{2+} comprised on average only 2%.

The five-day backward trajectories and the spatial distributions of CO and black carbon biomass emissions averaged over the previous five days prior to the flight is shown in Figure 11. Also shown are the urban/industrial emissions of SO_2 and NO_x , based on the inventory of Streets et al. [2002]. Note that at low altitudes, where the plume was detected, the trajectories come from a more westerly direction. We conclude from Figure 11 that the intercepted large plume

originates mainly from China coastal regions. The observed dust (Ca^{2+}) may be from mixing with higher altitude air originating from the more arid regions of Mongolia and Russia, or more localized sources of Ca^{2+} associated with the urban regions (e.g., cement production, construction, etc).

Comparing the predicted emissions of black carbon and CO for this plume to those of the 'pure' plume in Figure 7, Case 1, shows that the 'pure' biomass emissions were orders of magnitude higher, however concentrations of CO and absorbing fine particles, and other species associated with biomass burning, are much higher in this Yellow Sea plume. It may be that this plume is much closer to the source, is fresher, and thus less diluted. Or, that there are other major sources for these species, apart from biomass burning of field or forest residue.

The high concentrations of K^+ in this plume are hard to explain based on the burning of agricultural residues (emissions shown in Figure 11). One source may be that the K^+ comes from biofuel emissions. Although biofuel burning is estimated to account for less than 10% of the total global emission of K^+ [Andreae and Merlet, 2001], in China, roughly one-quarter of the energy use depends on biofuel [Streets et al., 1998]. These emissions are not shown in Figure 11. Urban biofuel emissions combined with large anthropogenic sources of SO_2 and NO_x , could lead to the observed high levels of ammonium sulfate and nitrate salts, and K^+ . Alternatively, an unusually large industrial source for K^+ in this region cannot be ruled out.

Case 3: Flight 19, Sea of Japan mixed biomass – pollution plume. The flight 19 plume intercepted in the Sea of Japan, (Figure 1) is apparently also a mix of biomass and fossil fuel emissions. The ionic composition of the plume is shown in Figure 12. K^+ and SO_4^{2-} are also correlated in this plume, ($r^2= 0.61$) suggesting the sources are well mixed. All concentrations are lower in this case, and K^+ concentrations are the lowest of our three Case studies. The NH_4^+/SO_4^{2-} molar ratio ranges between 2 and 3, the NO_3^-/SO_4^{2-} ratio is between 0.5-1, more typical of the plumes measured during TRACE-P. Much of the NO_3^- is apparently NH_4NO_3 since the averaged ratio of $NH_4^+/(SO_4^{2-} + NO_3^-)$, in equivalence, is 0.91. The measured ions also tend to balance. The ratio of the charge balance to total ion concentration is less than 1%. Similar to the Yellow Sea plume, backward trajectories (Figure13) show that the air mass associated with this plume apparently passed over northeast and eastern coastal regions in China, and along the west coast of the Yellow Sea. It then moved over the Yellow Sea, South Korea, and entered the Sea of Japan where it was intercepted.

Finally, for the three Case Studies, it is noted that the ratio of $SO_4^{2-}/(SO_2+SO_4^{2-})$ can serve as a measure of plume age. The observations in the cases studied generally confirm this. Back trajectories suggest the pure biomass plume of Flight 10 had traveled the greatest distance, and that the Flight 14 plume was the closest to the source. Flight 19 was likely only slightly more aged than Flight 14. The ratio of $SO_4^{2-}/(SO_2+SO_4^{2-})$ for the Flight 10 is 0.89 pptv/pptv, much

higher than those from Flight 14 at 0.4, and Flight 19 at 0.5 pptv/pptv (see Table 2).

3.3 Chemical relationships between biomass burning aerosols and relevant gases, and the contribution of biomass burning to mixed plumes.

To compare our observations to other studies, and to investigate the relative contribution of biomass (or biofuel) burning in the observed Asian outflow, the TRACE-P measurements that were apparently influenced by some form of biomass or biofuel burning are selected for more detailed analysis. This data set collects measurements from all research flights from plumes with at least five continuous measurements of K^+ above the PILS LOD, and with a plume maximum K^+ concentration higher than 200 pptv. This produces a data set of 153 points (each a 4 -minute average), comprising approximately 11% of all the data. If K^+ is only from biomass or biofuel combustion (which our analysis has suggested), and ignoring K^+ loss due to wet scavenging, this suggests that approximately at least 11% of the measurements of fine particles in the Asian outflows detected during TRACE-P were influenced by biomass or biofuel emissions.

For this selected data set the following is observed; 1) K^+ has the highest correlation with NH_4^+ ($r^2 = 0.827$) and absorbing aerosols (EC) ($r^2 = 0.804$), 2) K^+ is fairly well correlated with CO ($r^2 = 0.746$) and NO_3^- ($r^2 = 0.720$), and 3) K^+ has no obvious correlation with SO_4^{2-} with a r^2 of 0.334. No correlation between K^+

and Na^+ , Cl^- , or Ca^{2+} ($r^2 = 0.009, 0.011, 0.048$ respectively) suggests that the fine potassium was not associated with sea-salt or dust. Note that based on Ca^{2+} concentrations, only the Flight 16 plume is significantly affected by dust, the others show little or no dust contributions.

With the exception of the lower latitude measurement of flight 9 and 10, (Flight 10 is discussed in Case 1), most of the plumes containing K^+ appear to be mixed with fossil fuel emissions (SO_4^{2-}). This may result from the use of biofuel in the urban areas and/or merging of biomass burning and urban plumes. It is noted that the biomass burning - fossil fuel mixed plumes tend to be found at low altitudes and at latitudes greater than 30°N , and the relative pure biomass burning plumes tend to appear at higher altitudes and lower latitudes.

The general relationship between biomass burning aerosols and related gases are investigated using this data set and the results compared with findings from other field studies. The results are summarized in Tables 1 and 2. Because of the influence of background concentrations, the difference between plume and background concentrations (Δ) is used in the following analysis.

K⁺/CO ratios: Comparisons to other studies. Because other studies have reported the ratio of K^+/CO , we do a similar analysis for comparison. In a pure biomass plume, this ratio can provide some indication of the fine particle K^+ emission rate for a specific plume. In aged plumes, it could provide insight into the degree of wet deposition of the fine particles since the K^+ would be removed

more efficiently than the CO. However, in plumes of mixed biomass – fossil fuel burning the K^+/CO ratio could be much lower due to fossil fuel sources for CO.

Andreae et al. [1988, 1996] reported dK^+/dCO ratios of 1.3 to 4.9 pptv/ppbv for ambient particulate K^+ in biomass burning emissions from field measurements over Amazonia and Savanna. Reiner et al. [2001] give a value of 2.9 pptv/ppbv for plumes influenced by biomass emissions originated from northern India and transported over the Bay of Bengal to the measurement area south of India. Our data is generally within this range. Derived from the linear regression slope, for TRACE-P plumes containing some level of K^+ , dK^+/dCO range's from 1.5 to 4.55 pptv/ppbv, with the highest ratio from the highly polluted flight 14, Case 2 plume, and the lowest from flight 19, Case 3 plume, see Tables 1 and 2. The overall ratio dK^+/dCO for all TRACE-P plumes with K^+ is 3.67 pptv/ppbv.

Purity of biomass plumes: dCH_3Cl/dCO . In TRACE-P we recorded dCH_3Cl/dCO ranging from 0.2 to 0.88 pptv/ppbv, with the highest value from flight 10, the purest biomass plume. The overall ratio of dCH_3Cl/dCO for all selected biomass plumes is 0.33 pptv/ppbv, significantly lower than the 'pure' plume. From other studies, the ratio dCH_3Cl/dCO for fresh pure biomass burning smoke is usually 0.8 -1.1 pptv/ppbv [Andreae et al., 2001]. A value of 0.95 ± 0.01 pptv/ppbv is reported for a Southern Africa fire [Andreae et al. 1996]. Blake et al. [1996] report 0.85 ± 0.06 pptv/ppbv for the fairly fresh plumes from Brazilian emissions. Only our 'pure' biomass plume of Flight 10 (Case 1), with

$d\text{CH}_3\text{Cl}/d\text{CO} = 0.87 \text{ pptv/pptv}$ is in this range, suggesting that it is a relatively pure biomass plume. $d\text{CH}_3\text{Cl}/d\text{CO}$ ratios for the mixed plumes of Cases 2 (0.27) and 3 (0.33), are considerably less, consistent with mixed plumes of biomass and urban/industrial sources (Table 2).

$\text{K}^+/\text{SO}_4^{2-}$, $\text{CH}_3\text{Cl}/\text{CO}$, $\text{C}_2\text{Cl}_4/\text{CO}$ and SO_2/CO . Percentage contribution of biomass in mixed plumes

To estimate the contribution of biomass burning to the Asian outflow, we investigate the ratio of fine particulate $\text{K}^+/\text{SO}_4^{2-}$ for estimating the biomass contribution in a mixed plume. This ratio may be of interest since it is based solely on fine particle ionic composition and is thus more readily measured than some of the gases and organic aerosol components. The assumption is that biomass burning is the only source for fine potassium, and most of the sulfate comes from fossil fuel emissions. This will not apply to other regions where additional sources of fine K^+ exist.

Certain gaseous species can also provide clues to distinguish emissions from biomass burning and fossil fuels. For example, C_2Cl_4 may serve as a marker for urban/industrial emissions [Blake et al., 1999]. Nearly 93% of C_2Cl_4 is emitted in the Northern Hemisphere. Talbot et al. [1996] observed enhancements of C_2Cl_4 downwind of the highly urbanized east coast of Brazil. Thus, $\text{C}_2\text{Cl}_4/\text{CO}$ can provide a scale for urban/industrial influence. In contrast, since CH_3Cl can serve as biomass burning tracer, $\text{CH}_3\text{Cl}/\text{CO}$ indicates the degree of biomass

influence. Together, these ratios may provide a measure of relative emissions from fossil fuel and biomass burning.

Ratios of SO_2 and CO can also serve as a biomass burning/fossil fuel indicator. In the absence of volcanic emissions, SO_2 is mainly from anthropogenic burning of fossil fuel, with only a few percent from biomass burning [Chin et al., 1996]. This is consistent with our observations of low SO_4^{2-} concentrations in the 'pure' biomass plume of flight 10. CO is produced from both biomass burning and inefficient fossil fuel combustion.

To assess the utility of $dK^+/d\text{SO}_4^{2-}$, it is compared to these gas phase ratios. This analysis is to test the general trend of the whole data set. The number of selected data points for each plume, data merging method, and the linear correlation coefficient of each plume all affect the overall relationship.

In TRACE-P, $dK^+/d\text{SO}_4^{2-}$ ranges from the highest, 2.37 pptv/pptv (flight 10), to the lowest of 0.16 pptv/pptv (flight 19). The overall ratio for the TRACE-P data set having any evidence of biomass burning is 0.24 pptv/pptv, which is comparable to other studies which report 0.153 pptv/pptv [Novakov et al., 2000] and 0.181 pptv/pptv [Reiner et al., 2001] for measurements made during the India Ocean Experiment (INDOEX). A ratio of 4.57 pptv/pptv is found for biomass burning in Brazil [Ferek et al., 1998].

To investigate the fossil fuel influence on the ratio of $dK^+/d\text{SO}_4^{2-}$, this ratio is compared to $d\text{C}_2\text{Cl}_4/d\text{CO}$. The result is shown in Figure 14, where each point represents one TRACE-P plume. The ratio in each plume was determined from

linear regression. To assess the goodness of this fit, the r^2 of each plume is compared with the Pearson's correlation coefficient critical value [Meddis, 1975]. The solid data points in Figure 14 are those plumes where the r^2 is higher than the critical correlation coefficient value, while the open circle points have either dK^+/dSO_4^{2-} or dC_2Cl_4/dCO , or both with r^2 lower than the critical value. The linear regression line in Figure 14 is only based on those data whose r^2 is higher than the critical value (solid dots). As expected, dK^+/dSO_4^{2-} is anti-correlated with dC_2Cl_4/dCO , consistent with a smaller influence of fossil fuel combustion for higher dK^+/dSO_4^{2-} ratios. A similar correlation analysis could be done between dK^+/dSO_4^{2-} and dCH_3Cl/dCO , however the results are poor. This is consistent with our observations discussed above, that CH_3Cl is not as well correlated with CO as K^+ .

Ratios of dSO_2/dCO have also been used for estimating the extend of biomass burning influence. In TRACE-P, dSO_2/dCO ranges from 0.33 pptv/ppbv to 20.05 pptv/ppbv. The overall ratio of for plumes with some biomass burning is 9.98 pptv/ppbv. The ratio of total sulfur to CO, $(dSO_4^{2-} + dSO_2)/dCO$, is more preferable since at times SO_4^{2-} can account for a large portion of the total sulfur. In TRACE-P, sulfate can account for as high as 89% of the total sulfur (shown in Table 2). In general $(dSO_4^{2-} + dSO_2)/dCO$ ratios range from 3.65 pptv/ppbv to 37.48 pptv/ppbv, and the overall ratio for all plumes with some biomass burning is 17.17 pptv/ppbv. This value is similar to the ratio

reported by Reiner et al. [2001] for a mixed plume over the Indian Ocean (see Table 1).

For relatively pure biomass burning emissions from previous field and laboratory studies, typical $d\text{SO}_2/d\text{CO}$ ratios are between 2 and 5 pptv/ppbv, which also agrees with our measurements (Table 1). The ratio of $d\text{SO}_2/d\text{CO}$ can also be determined from emission inventories (in this case the ratio is SO_2/CO). Formenti et al. [2001] reports a SO_2/CO molar ratio for fossil fuel pollution in eastern Europe of 50 pptv/ppbv. Streets and Waldhoff et al., [1998, 1999] give a ratio of 42 pptv/ppbv for the India emission inventory, and Streets et al. [2002] also reports an Asian SO_2/CO ratio of 54 pptv/ppbv based on anthropogenic emission inventories.

Using the ranges of $d\text{SO}_2/d\text{CO}$ (or $d\text{SO}_y/d\text{CO}$) for different type of plumes, based on measurements and emission inventories, we may estimate the relative contribution of biomass burning to the CO concentration for these plumes. Since sulfate can account for a high percentage of the total sulfur during TRACE-P, we use $d\text{SO}_y/d\text{CO}$ ($\text{SO}_y = \text{SO}_2 + \text{SO}_4^{2-}$) instead of $d\text{SO}_2/d\text{CO}$. To estimate the percent contribution we use a method similar to Formenti et al., [2001], where we assume that the $d\text{SO}_y/d\text{CO}$ molar ratio from fossil fuel emissions is 40 pptv/ppbv, and for pure biomass burning emissions the ratio is 5 pptv/ppbv. Then by assuming a linear interpolation, the relative influence of biomass burning, or fossil fuel emissions, on CO for these plumes can be estimated. With this method, the percent biomass contribution is equal to 114.29

- $2.86 \cdot (dSO_y / dCO)$, for dSO_y / dCO between 5 and 40, and the ratio in units of pptv/ppbv.

Figure 15 shows the relationship between dK^+ / dSO_4^{2-} and the estimated biomass contribution based on the above method. The data in the figure includes all the selected TRACE-P plumes that were affected by both biomass burning and fossil fuel emissions. dK^+ / dSO_4^{2-} is positively correlated with the estimated biomass contribution with a r^2 of 0.64 (data points which have r^2 lower than the critical value are excluded).

Data from other studies are also plotted in Figure 15. For INDOEX (Indian Ocean Experiment), the biomass contribution to CO is calculated based on dSO_2 / dCO and dSO_4^{2-} / dCO ratio provided in Reiner et al. (2001) (to calculate dSO_y / dCO), and dK^+ / dSO_4^{2-} is calculated based on data in the paper. The INDOEX result is influenced by both biomass and fossil fuel burning and tends to fit with the TRACE-P results.

For relatively pure biomass plumes, dK^+ / dSO_4^{2-} can be extremely high and not fit with the general trend of Figure 15. For example, for the TRACE-P 'pure' biomass plume (Flight 10) dK^+ / dSO_4^{2-} is 2.37 pptv/ppbv which does not fit with the other points. Furthermore, the linear correlation coefficient in this plume is lower than the critical correlation coefficient value. In another study of biomass burning fires, called Smoke, Clouds, and Radiation – Brazil (SCAR-B), a similar result is observed (see Figure 15). This is based on the data provided in

Ferek et al. [1998], which we use to estimate dK^+/dSO_4^{2-} (4.64 pptv/pptv) and dSO_2/dCO (2.7 pptv/ppbv).

For plumes mainly composed of fossil fuel emissions, the ratio of dK^+/dSO_4^{2-} for TRACE-P data goes as low as 0.16 pptv/pptv. Gabriel et al. [2002] also reports a low ratio of 0.07 pptv/pptv for the aerosols from Arabia, with strong influence from fossil fuel.

Combining measurements of dK^+/dSO_4^{2-} and Figure 15 allows prediction of the percent contribution of CO to the biomass plume. However, by considering only the fine particle data, the ratio of dK^+/dSO_4^{2-} may be used directly to crudely estimate the relative contributions of biomass and fossil fuel emissions to the fine particle mass. This approach is tested on the three case studies investigated above. To do this we assume that dK^+/dSO_4^{2-} is equal or less than 0.1 pptv/pptv for plumes with little biomass influence (assume 10%), and is equal or larger than 0.7 pptv/pptv for pure biomass plumes. Since the overall ratio of dK^+/dSO_4^{2-} for the TRACE-P mixed biomass plumes is 0.24 pptv/pptv, this method suggests that on average $30 \pm 5\%$ of the fine particle aerosol mass in the TRACE-P plumes is from biomass burning emissions. For the three case studies, we estimate that roughly $100\% \pm 15\%$ (Case 1, Flight 10), $62 \pm 10\%$ (Case 2, Flight 14), and $18 \pm 2\%$ (Case 3, Flight 19) of the fine particle mass is from a biomass influence.

Applying this technique to all TRACE-P mixed plumes, the spatial distribution of the percent biomass contribution to plumes can be crudely

estimated. Plotted in Figure 16, most of the biomass contribution occurs at lower latitudes and the mixed plumes more often appear near northern coastal areas near China, Korea, and Japan.

In order to test whether this method is reasonable, results from previous studies are compared with estimates using other methods. Novakov et al, (2000) estimated that biomass combustion accounted for about 20% of the aerosol mass, based on carbonaceous aerosol concentration ratios measured during INDOEX. Using data from the paper to estimate dK^+/dSO_4^{2-} gives a ratio of $17 \pm 2\%$ from biomass burning. Also from INDOEX, Reiner et al. (2001) reported that $30 \pm 10\%$ of the aerosol mass was due to biomass emissions for the northern Indian Ocean region. We calculate dK^+/dSO_4^{2-} ratios from the reported data, and obtain a value of $21 \pm 2\%$ of aerosol mass from biomass contribution. Thus results from the dK^+/dSO_4^{2-} ratio are consistent with other methods for determining biomass contributions in mixed plumes. One must keep in mind that these are crude estimations and many factors can cause uncertainties in the predicted contributions.

In summary, the three case studies presented encompass the range of ratios discussed in Table 1. The plumes from Flights 10, 14, and 19 (Cases 1, 2, and 3) are all influenced by biomass emissions and represent cases that are nearly pure biomass, moderately influenced, and not greatly influenced by biomass emissions. This is consistently observed by a number of ratios. Higher values of dK^+/dSO_4^{2-} and dCH_3Cl/dCO correspond with plumes with highest

contributions of biomass emissions. Conversely, higher ratios of dC_2Cl_4/dCO , dSO_2/dCO , and $(dSO_2+dSO_4^{2-})/dCO$ correspond to plumes of lower biomass and higher fossil fuel burning influence.

CONCLUSIONS

In Asian outflow plumes measured from the NASA P-3B research aircraft during TRACE-P, fine particle potassium (K^+) concentrations can serve as a biomass burning tracer. For all research flights based out of Hong Kong, China, and Yakota Air Force Base, Japan, K^+ is correlation with optically absorbing particles ($r^2=0.73$), ammonium ($r^2=0.77$), and CO ($r^2=0.61$). Overall, the K^+ - CO correlation is higher than that between methylchloride (CH_3Cl) and CO ($r^2 = 0.50$), a commonly used gaseous biomass tracer. No correlations between fine K^+ and sodium or calcium indicate that sea salt and dust make little contributions to the observed K^+ , and most of the optically absorbing particles were likely soot.

Based on concentrations of fine particle potassium and sulfate, most of the plumes intercepted are influenced by both biomass burning and fossil fuel emissions. Fine particle potassium data suggests that some form of biomass emissions influenced approximately 10% of the TRACE-P measurements of Asian outflows.

Purest biomass burning plumes were encountered in the lower latitudes between approximately 15 and 25°N and were found in layers at altitudes from 2 to 4 km asl, separated from the boundary layer. For the one plume studied in

detail, the biomass plume was situated over a pollution plume, containing high sulfate, in the boundary layer. Backward trajectories combined with fire map data suggest the biomass plume originated from burning in Thailand. In this relatively pure biomass plume concentrations of fine particle potassium, ammonium, nitrate and absorbing aerosol particles were all enhanced and highly correlated.

At latitudes higher than 25°N mixed biomass – fossil fuel plumes were observed in the marine boundary layer. A plume containing the studies highest concentrations of sulfate, nitrate, potassium, and CO was observed in the Yellow Sea. This unique plume may have resulted from a combination of fossil fuel and biofuel emissions from the large cities, possibly Beijing, located on the western edge of the Yellow Sea. This plume is contrasted to one observed in the Sea of Japan. It contained some evidence of biomass burning, but was comprised mainly of fossil fuel emissions.

The chemical characteristics of the biomass plumes are investigated through ratios of various components. K^+/CO ratios were typically between 1.4 to 4.6 pptv/ppbv, similar to those from other studies. Comparison's with other biomass burning and fossil fuel emission indicators, such as CH_3Cl/CO , C_2Cl_4/CO and SO_2/CO indicate that the molar ratio of fine particle dK^+/dSO_4^{2-} can be used to estimate the relative influence of biomass burning on fine particle mass in mixed plumes. It is estimated that on average, approximately $30 \pm 5\%$ of the aerosol mass in the mixed plumes observed during TRACE-P was from some

form of biomass burning emissions. For the plumes investigated in detail, the large Yellow Sea plume was approximately $62 \pm 10\%$ from biomass/biofuel combustion, and the Sea of Japan plume was $18 \pm 2\%$. Comparison of these estimates to model predictions would provide a further test of the utility of this approach.

ACKNOWLEDGEMENTS

The authors gratefully acknowledge the support of the National Atmospheric and Space Administration (NASA) under grant number NCC-1-411L. We also thank the personnel of the NASA Wallops Flight Facility for all their help during the experiment.

REFERENCES

- Andreae, M. O., Soot carbon and excess fine potassium: Long - range transport of combustion-derived aerosols, *Science*, 220, 1148-1151, 1983
- Andreae, M. O., et al., Biomass burning emissions and associated haze layers over Amazonia, *J. Geophys. Res.*, 93,1509-1527, 1988
- Andreae, M. O., Biomass burning: Its history, use, and distribution and its impact on environmental quality and global climate, in Global biomass burning: atmospheric, climatic, and biospheric implications, edited by J. S. Levine, 1-21, MIT press, Cambridge, Mass., 1991

- Andreae, M. O., E. Atlas, H. Cachier, W. R. Cofer III, G. W. Harris, G. Helas, R. Koppmann, J.-P. Lacaux, and D. E. Ward, Trace gas and aerosol emissions from savanna fires, in *Biomass Burning and Global Change*, Vol. 1., edited by J. S. Levine, 278-295, MIT press, Cambridge, Mass., 1996
- Andreae, M. O., P. Artaxo, H. Fischer, S. R. Freitas, J.-M. Gregoire, A. Hansel, P. Hoor, R. Kormann, R. Krejci, L. Lange, J. Lelieveld, W. Lindinger, K. Longo, W. Peters, M. deReus, B. Scheeren, M. A. F. Silva Dias, J. Strom, P. F. J. Van Velthoven, and J. Williams, Transport of biomass burning smoke to the upper troposphere by deep convection in the equatorial region, *Geophys. Res. Lett.*, 28, 951-954, 2001
- Andreae, M. O. and P. Merlet, Emission of trace gases and aerosols from biomass burning, *Global Biogeochemical Cycles*, 15, 955-966, 2001
- Blake, N. J., D. R. Blake, B. C. Sive, T.-Y. Chen, F. S. Rowland, J. E. Collins, Jr., G. W. Sachse, and B. E. Anderson, Biomass burning emissions and vertical distribution of atmospheric methyl halides and other reduced carbon gases in the South Atlantic region, *J. Geophys. Res.*, 101, 24,151-24,164, 1996
- Blake, N. J., D. R. Blake, T.-Y. Chen, J. E. Collins, Jr., G. W. Sachse, B. E. Anderson, and F. S. Rowland, Distribution and seasonality of selected hydrocarbons and halocarbons over the western Pacific basin during PEM-West A and PEM-West B, *J. Geophys. Res.*, 102, 28,315-28,331, 1997
- Blake, N. J., D. R. Blake, O. W. Wingenter, B. C. Sive, L. M. McKenzie, J. P. Lopez, I. J. Simpson, H. E. Fuelberg, G. W. Sachse, B. E. Anderson, G. L. Gregory,

- M. A. Carroll, G. M. Albercook, F. S. Rowland, Influence of southern hemispheric biomass burning on midtropospheric distributions of nonmethane hydrocarbons and selected halocarbons over the remote South Pacific, *J. Geophys. Res.*, 104, 16,213-16,232, 1999
- Bond, T. C., T. L. Anderson, and D. Campbell, Calibration and Intercomparison of filter-based measurements of visible light absorption by aerosols, *Aerosol Sci. Technol.*, 30, 582-600, 1999
- Cachier, H., J. Ducret, M.-P. Bremond, V. Yoboue, J.-P. Lacaux, A. Gaudichet, and J. Baudet, Biomass burning in a savanna region of the Ivory Coast, in Global Biomass Burning: Atmospheric Climatic and Biospheric Implications, edited by J. S. Levine, pp. 174-180, MIT press, Cambridge, Mass., 1991
- Chin, M., D. J. Jacob, G. M. Gardner, M. S. Foreman-Fowler, P. A. Spiro, and D. L. Savoie, A global three-dimensional model for tropospheric sulfate, *J. Geophys. Res.*, 101, 18,667-18,690, 1996
- Crutzen, P. J. and M. O. Andreae, Biomass burning in the tropics: Impact on atmospheric chemistry and biogeochemical cycles, *Science*, 250, 1669-1678, 1990
- Dibb, J. E., R. W. Talbot, B. L. Lefer, E. Scheuer, G. L. Gregory, E. V. Browell, J. D. Bradshaw, S. T. Sandholm, and H. B. Singh, Distribution of beryllium 7 and lead 210, and soluble aerosol-associated ionic species over the western Pacific: PEM West B, February-March 1994, *J. Geophys. Res.*, 102, 28,287-28,302, 1997

- Ferek, R. J., J. S. Reid, P. V. Hobbs, D. R. Blake, and C. Lioussé, Emission factors of hydrocarbons, halocarbons, tracer gases and particles from biomass burning in Brazil, *J. Geophys. Res.*, 103, 32,107-32,118, 1998
- Formenti, P., T. Reiner, D. Sprung, M. O. Andreae et al., The STAAARTE-MED 1998 summer airborne measurements over the Aegean Sea: I. Aerosol particles and trace gases, *J. Geophys. Res.*, submitted, 2001
- Fuelberg, H. E., R. O. Loring, Jr., M. V. Watson, M. C. Sinha, K. E. Pickering, A. M. Thompson, D. P. McNamara, G. W. Sachse, D. R. Blake, and M. R. Schoeberl, TRACE-A trajectory intercomparison: Part 2. Isentropic and kinematic methods. *J. Geophys. Res.*, 101, 23,927-23,939, 1996
- Gabriel, R., O. L. Mayol-Bracero, and M. O. Andreae, Chemical characterization of submicron aerosol particles collected over the Indian Ocean, *J. Geophys. Res.*, 107, INX2-4, 2002
- Gaudichet, A., F. Echalar, B. Chatenet, J. P. Quisefit, G. Malingre, H. Cachier, P. Buat-Menard, P. Artaxo, and W. Maenhaut, Trace elements in tropical African savanna biomass burning aerosols, *J. Atmos. Chem.*, 22, 19-39, 1995
- Lacaux J. P., et al., Biomass burning in the tropical savannas of Ivory Coast: An overview of the field experiment Fire of Savannas (FOS/DECAFE 91), *J. Atmos. Chem.*, 22, 195-216, 1995
- Ma, Y., R. J. Weber, K. Maxwell, D. A. Orsini, Y.-N. Lee, B. J. Huebert, S. G. Howell, T. Bertram, R. W. Talbot, J. E. Dibb, and E. Scheuer, Intercomparisons

- of airborne measurements of fine particle ionic chemical composition during TRACE-P and ACE-Asia. *J. Geophys. Res. ACE-Asia special issue*, 2002
- Meddis, R., Statistical handbook for non-statisticians, McGraw-Hill book company, Berkshire, England, 1975
- Novakov, T., M. O. Andreae, R. Gabriel, T. W. Kirchsteter, O.L. Mayol-Bracero, and V. Ramanathan, Origin of carbonaceous aerosols over the tropical Indian Ocean: Biomass burning or fossil fuels?, *Geophys. Res. Lett.*, 27, 4061-4064, 2000
- Orsini, D., Y. Ma, A. Sullivan, B. Sierau, K. Baumann and R. J. Weber, Refinements to the particle-into-liquid sampler (pils) for ground and airborne measurements of water-soluble aerosol chemistry, *Atmos. Environ.* Submitted, 2002
- Reiner, T., D. Sprung, C. Jost, R. Gabriel, O. L. Mayol-Bracero, M. O. Andreae, T. L. Campos and R. E. Shetter, Chemical characterization of pollution layers over the tropical Indian Ocean: Signatures of emissions from biomass and fossil fuel burning, *J. Geophys. Res.*, 106, 28,497-28,510, 2001
- Sachse, G. W., J. E. Collins Jr., G. F. Hill, L. O. Wade, L. G. Burney, and J. A. Ritter, Airborne tunable diode laser system for high precision concentration and flux measurements of carbon monoxide and methane, *Proc. SPIE int. Opt. Eng.*, 1433, 145-156, 1991
- Schauer, J. J., W. F. Rogge, L. M. Hildemann, et al., Source apportionment of airborne particulate matter using organic compounds as tracers, *Atmos. Environ.* 30, 22, 3837-3855, 1996

- Sive, B. C., Atmospheric NMHCs: Analytical methods and estimated hydroxyl radical concentrations, Ph. D. thesis, Univ. of Calif. Irvine, 1998
- Streets, D. G., S. T. Waldhoff, Biofuel use in Asia and acidifying emissions, *Energy*, 23, 1029-1042, 1998
- Streets D. G., and S. T. Waldhoff et al., Greenhouse-gas emission from biofuel combustion in Asia, *Energy*, 24, 841-855, 1999
- Streets, D. G., T. C. Bond, G. R. Carmichael, S. Fernandes, Q. Fu, D. He, Z. Klimont, S. M. Nelson, N. Y. Tsai, M. Q. Wang, J.-H. Woo, and K. F. Yarber, An inventory of gaseous and primary aerosol emissions in Asia in the year 2000, *J. Geophys. Res.*, *TRACE-P special issue*, 2002
- Tabazadeh, A., M. Z. Jacobson, H. B. Singh, O. B. Toon, J. S. Lin, B. Chatfield, A. N. Thakur, R. W. Talbot and J. E. Dibb, Nitric acid scavenging by mineral and biomass burning aerosols, *Geophys. Res. Lett.*, 25: 4185-4188, 1998
- Talbot R. W. et al., Chemical characteristics of continental outflow over the tropical South Atlantic Ocean from Brazil and Africa, *J. Geophys. Res.*, 101, 24,187-24,202, 1996
- Thornton, D. C., A. R. Bandy, F. H. Tu, B. W. Blomquist, G. M. Mitchell, W. Nadler, and D. H. Lenschow, Fast Airborne Sulfur Dioxide Measurements by Atmospheric Pressure Ionization Mass Spectrometry (APIMS), *J. Geophys. Res.*, submitted, 2002

- Weber, R. J., D. A. Orsini, Y. Duan, Y.-N. Lee, P. J. Klotz, and F. Brechtel, A Particle-Into-Liquid Collector for Rapid Measurement of Aerosol Bulk Chemical Composition, *Aerosol Sci. Technol.*, 35, 718-727, 2001
- Weber, R. J., S. Lee, B. Wang, R. L. Mauldin, M. Zondlo, F. L. Eisele, K. Moore, V. Kapustin, and A. Clarke, Particle production within and near aged Asian anthropogenic plumes observed during TRACE-P, *J. Geophys. Res.*, *TRACE P special issue*, 2002

FIGURE CAPTIONS

- Figure 1. Flight paths of the NASA P3-B aircraft during TRACE-P, and fine particle potassium spatial distributions. The locations of three plumes discussed in detail are also shown.
- Figure 2. Vertical distribution of fine particle potassium in the Western Pacific during TRACE-P.
- Figure 3. Relationship between fine potassium and light absorbing aerosol particles (PSAP measurement) for all intensive flights shown in Figure 1. The insert is for potassium less than 1000 pptv.
- Figure 4. Relationship between fine potassium and carbon monoxide. The insert is for potassium less than 1000 pptv.
- Figure 5. Relationship between fine potassium and methyl chloride. The insert is for potassium less than 1000 pptv. Dashed lines are linear regressions for three arbitrary selected plumes during the study.
- Figure 6. Relationship between fine potassium and ammonium. The insert is for potassium less than 1000 pptv.
- Figure 7. Spatial distribution of biomass CO and black carbon emissions averaged over five-days prior to flight 10, and five-day back trajectories for the plumes encountered during flight 10.

- Figure 8. Aircraft altitude and fine particle ionic concentrations measured during flight 10, a relatively pure biomass plume from Thailand.
- Figure 9. Vertical profiles for various species measured in the region of the 'pure' biomass plume of flight 10. Closed circles are for leg 1, open triangles are for leg 2. A temperature inversion at ~ 2 km asl separates the biomass plume from the surface level pollution layer.
- Figure 10. Aircraft altitude and fine particle ionic composition in the Yellow Sea plume of flight 14, Case 2.
- Figure 11. Spatial distribution of biomass CO and black carbon emissions averaged over five-days prior to flight 14, and five-day back trajectories for the plumes encountered during flight 14. Anthropogenic SO₂ and NO_x emission sources for 2000 are also shown.
- Figure 12. Aircraft altitude and fine particle ionic composition in the Sea of Japan plume of flight 19, Case 3.
- Figure 13. The five-day back trajectories for the plume encountered during flight 19.
- Figure 14. Relationship between dK^+/dSO_4^{2-} and dC_2Cl_4/dCO for the biomass plumes encountered during TRACE-P. Each point indicates one plume. Empty circle means the correlation coefficient of the corresponding plume is lower than the critical correlation coefficient;

solid circles means the correlation coefficient is higher than the critical value. The linear regression is based only on the solid circles.

Figure 15. Relationship between dK^+/dSO_4^{2-} and the percentile of biomass contribution to CO for the biomass plumes encountered during TRACE-P. Results from previous studies. Are also included. The linear regression is based only on the TRACE-P plume solid circles.

Figure 16. Spacial distribution of the percent biomass contribution to the aerosol ionic mass concentration for the biomass plumes intercepted during TRACE-P.

Table 1. Results from linear regression analysis of the correlation among ambient aerosol components and gas species for this and other studies.

	This work	Other measurement
$\frac{dK^+}{dCO}$	Overall: 3.67 Max.: 4.55 (flight 14) Min.: 1.38 (flight 19) Average: 2.86	1.3-4.9 biomass burning, field [Andreae et al., 1988, 1996] 2.9 Indian ocean, field [Reiner et al., 2001]
$\frac{dCH_3Cl}{dCO}$	Overall: 0.33 Max.: 0.88 (flight 10, 16) Min.: 0.22 (flight 19) Average: 0.47	0.95 ± 0.01 Southern Africa, field [Andreae et al., 1996] 0.85 ± 0.06 Brazilian emissions, field [Blake et al., 1996]
$\frac{dSO_y}{dCO}$	dSO_2/dCO Overall: 9.98 Max.: 20.05 (flight 14) Min.: 0.33 (flight 10) Average: 8.33	$dSO_2/dCO = 6.5$ biomass burning fire, laboratory [Crutzen and Andreae, 1990] $dSO_2/dCO = 4.0$ biomass burning, field [Andreae et al., 1996]
	$(dSO_2 + dSO_4^{2-})/dCO$ Overall: 17.42 Max.: 37.48 (flight 16) Min.: 3.65 (flight 10) Average: 17.17	$dSO_2/dCO = 0.77$ biomass burning, field [Lacaux et al., 1995] $dSO_y/dCO = 2.4-6.5$ biomass burning, field [Andreae et al., 1988] $dSO_2/dCO = 7.8, dSO_4^{2-}/dCO = 16$ Indian ocean field [Reiner et al., 2001]
$\frac{dK^+}{dSO_4^{2-}}$	Overall: 0.24 Max.: 2.37 (flight 10) Min.: 0.15 (flight 16, 19) Average: 0.55	0.153 India field, [Novakov et al., 2000] ^a 0.181 Indian ocean field, [Reiner et al., 2001] ^a 4.639 Brazil biomass burning fires, [Ferek et al., 1998] ^a

Units: pptv/pptv for dK^+/dSO_4^{2-} , pptv/ppbv for else

Overall ratio is calculated by the whole selected biomass plumes dataset, while average ratio is the average of the corresponding ratios for all selected individual plumes.

^aCalculated based on the data provided in the paper

Table 2. Results from linear regression analysis for the correlation between various fine particle and gaseous species for the three selected case study plumes discussed in detail in the text.

	Flight10	Flight 14	Flight 19
$\frac{SO_4^{2-}}{SO_4^{2-} + SO_2}$	0.89	0.42	0.51
$\frac{dK^+}{dCO}$	2.02*	4.55	2.24
$\frac{dCH_3Cl}{dCO}$	0.87	0.27	0.33
$\frac{dC_2Cl_4}{dCO}$	-0.02	0.01	0.07
$\frac{dSO_2}{dCO}$	0.42*	10.28	12.36
$\frac{dSO_4^{2-} + dSO_2}{dCO}$	3.68*	19.22	26.46
$\frac{dK^+}{dSO_4^{2-}}$	2.37	0.49	0.16
% of biomass contribution	100	62±10	18±2

*r² lower than critical value, and calculated as $\Sigma(X/CO)/n$.

Units: pptv/ppbv for dX/dCO ($X = K^+, CH_3Cl, C_2Cl_4, SO_2, SO_4^{2-}$), and pptv/pptv for others

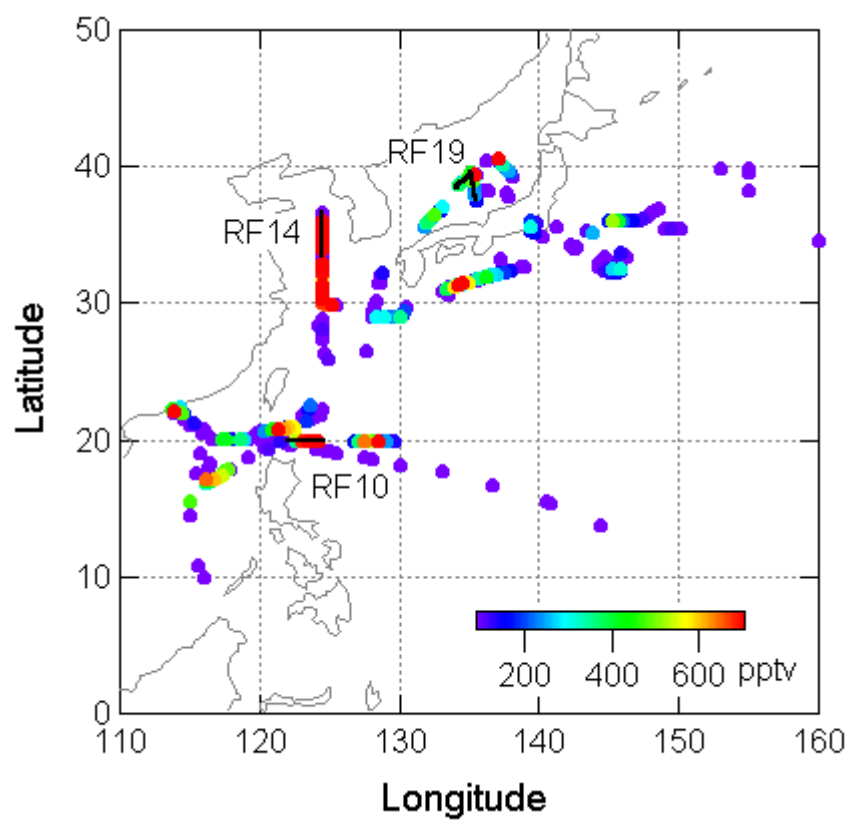


Figure 1

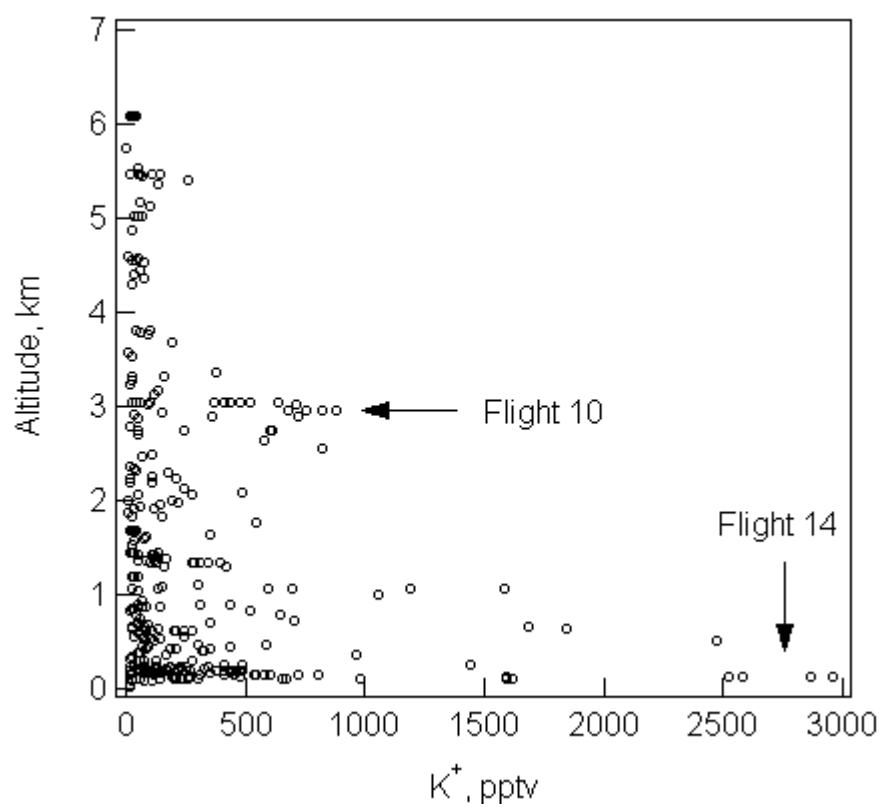


Figure 2

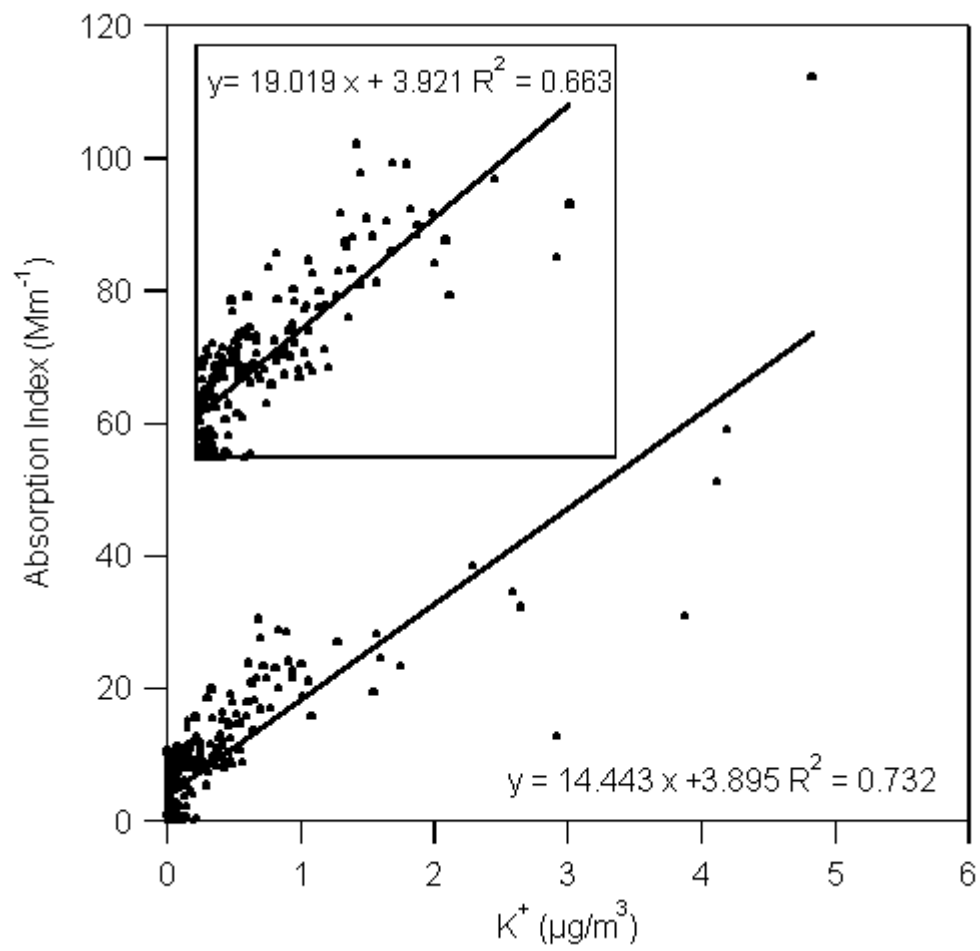


Figure 3

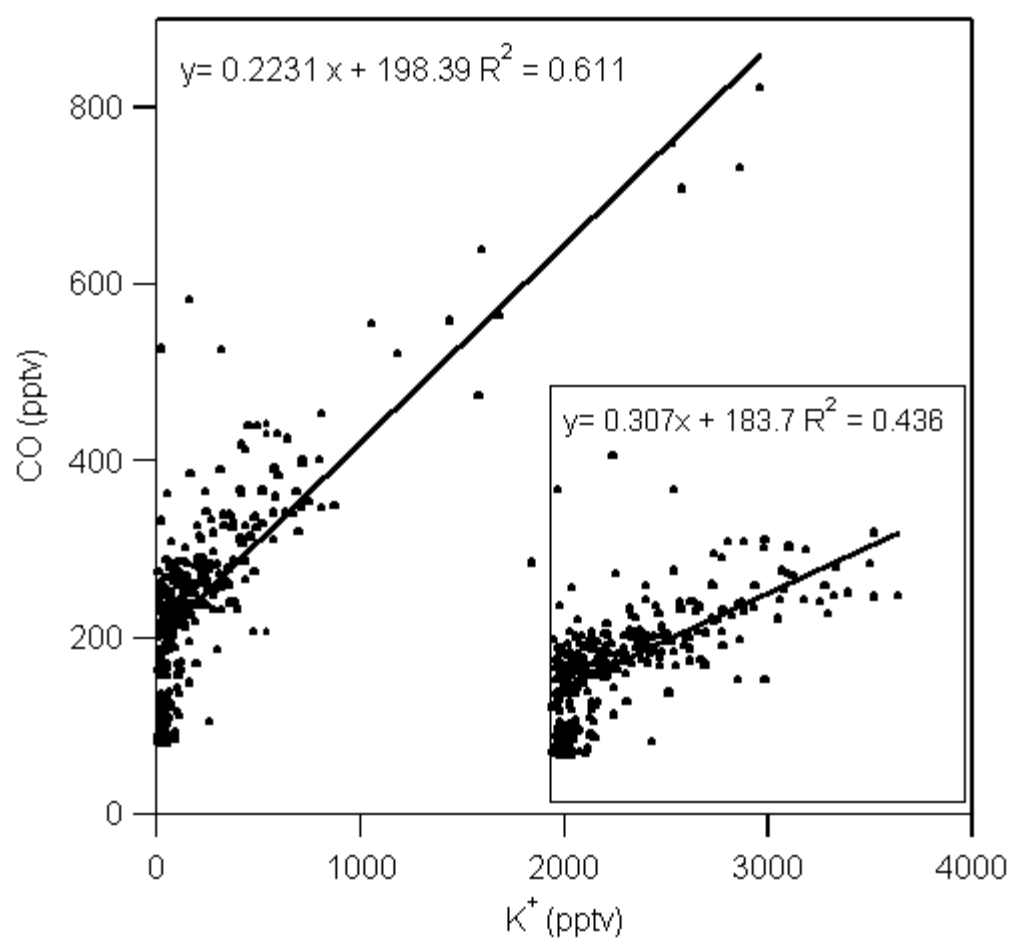


Figure 4

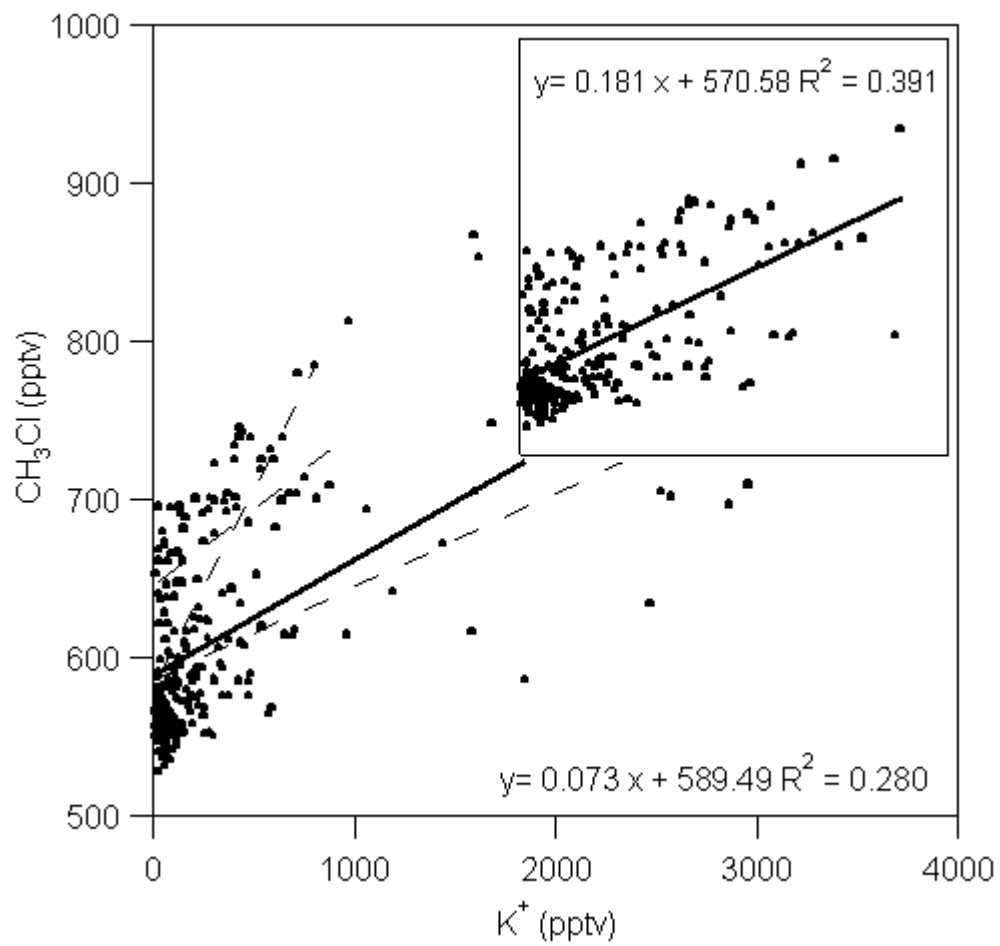


Figure 5

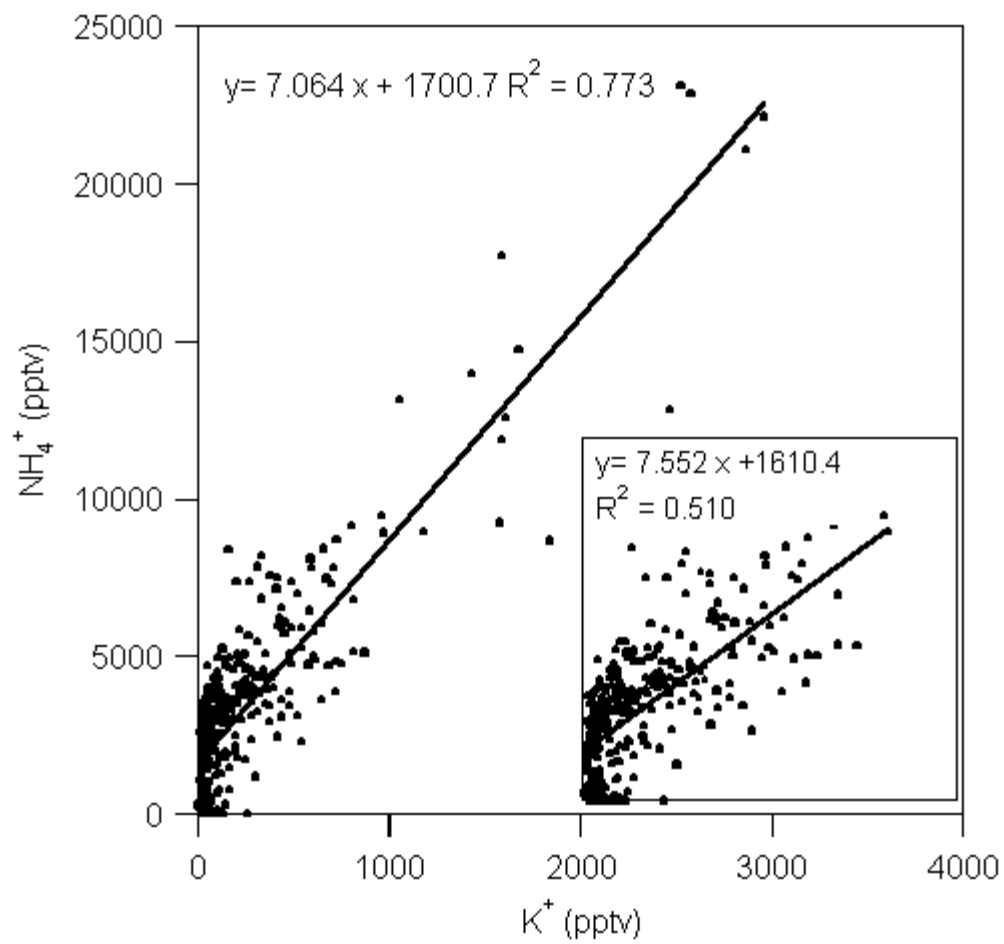


Figure 6

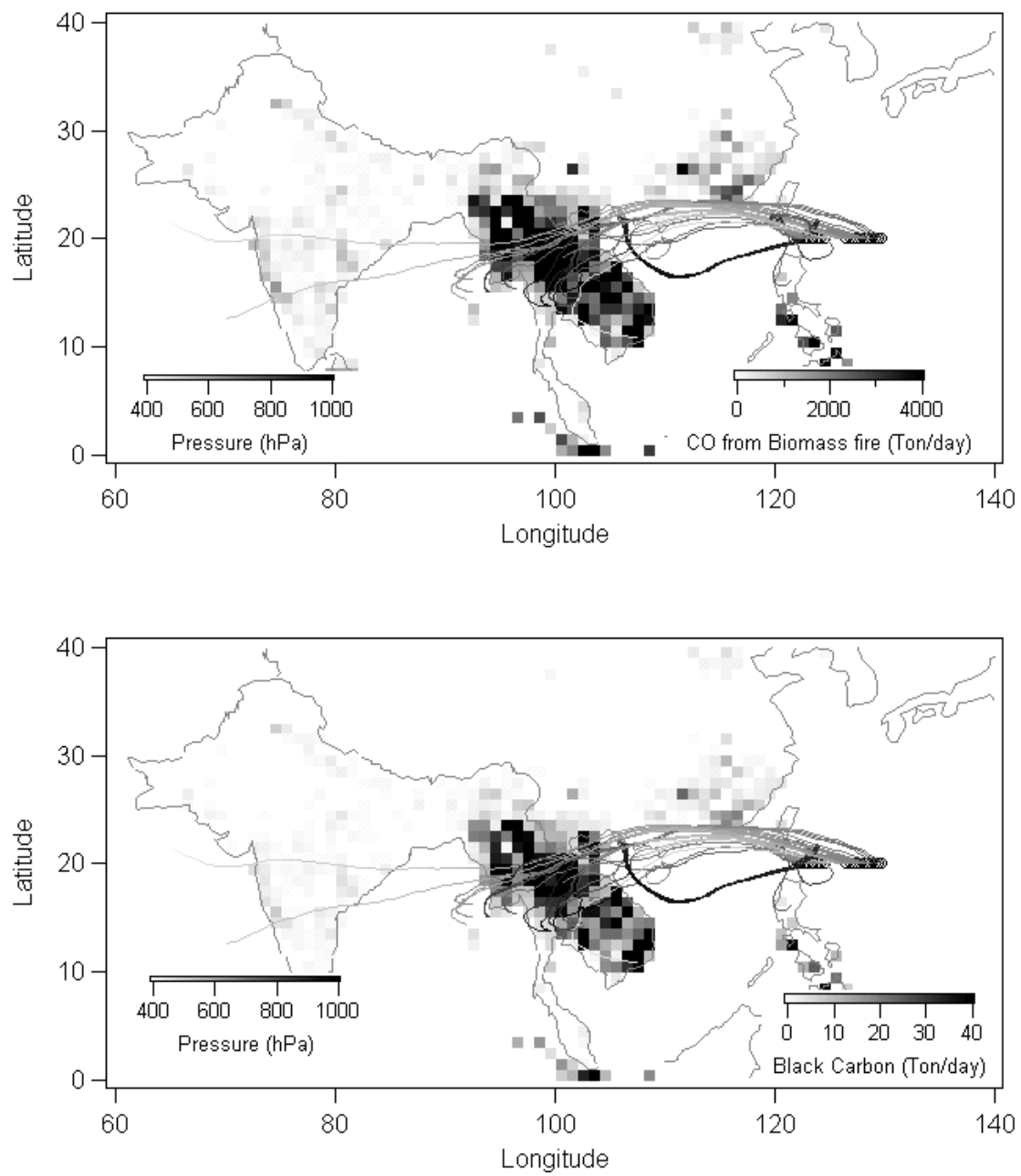


Figure 7

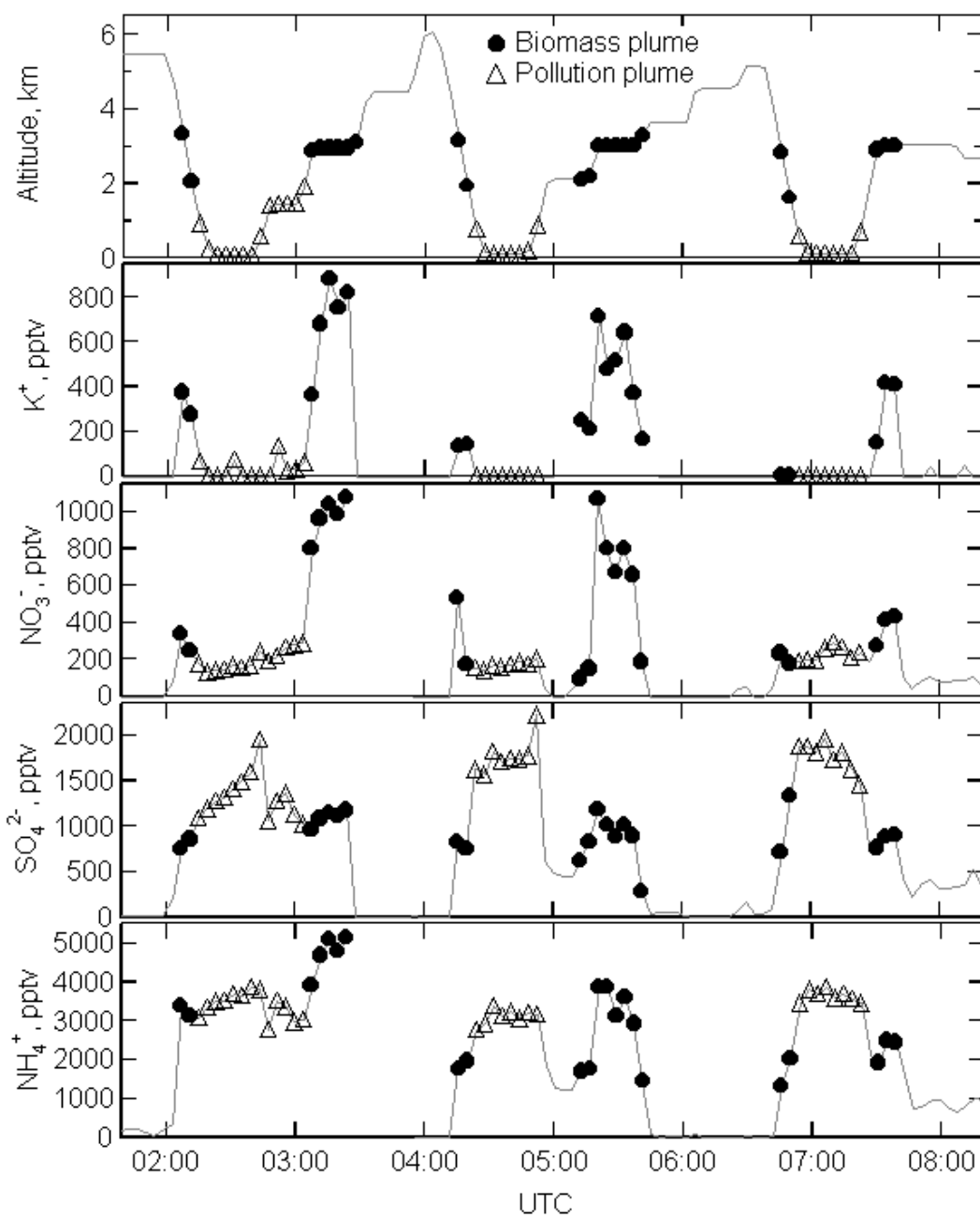


Figure 8

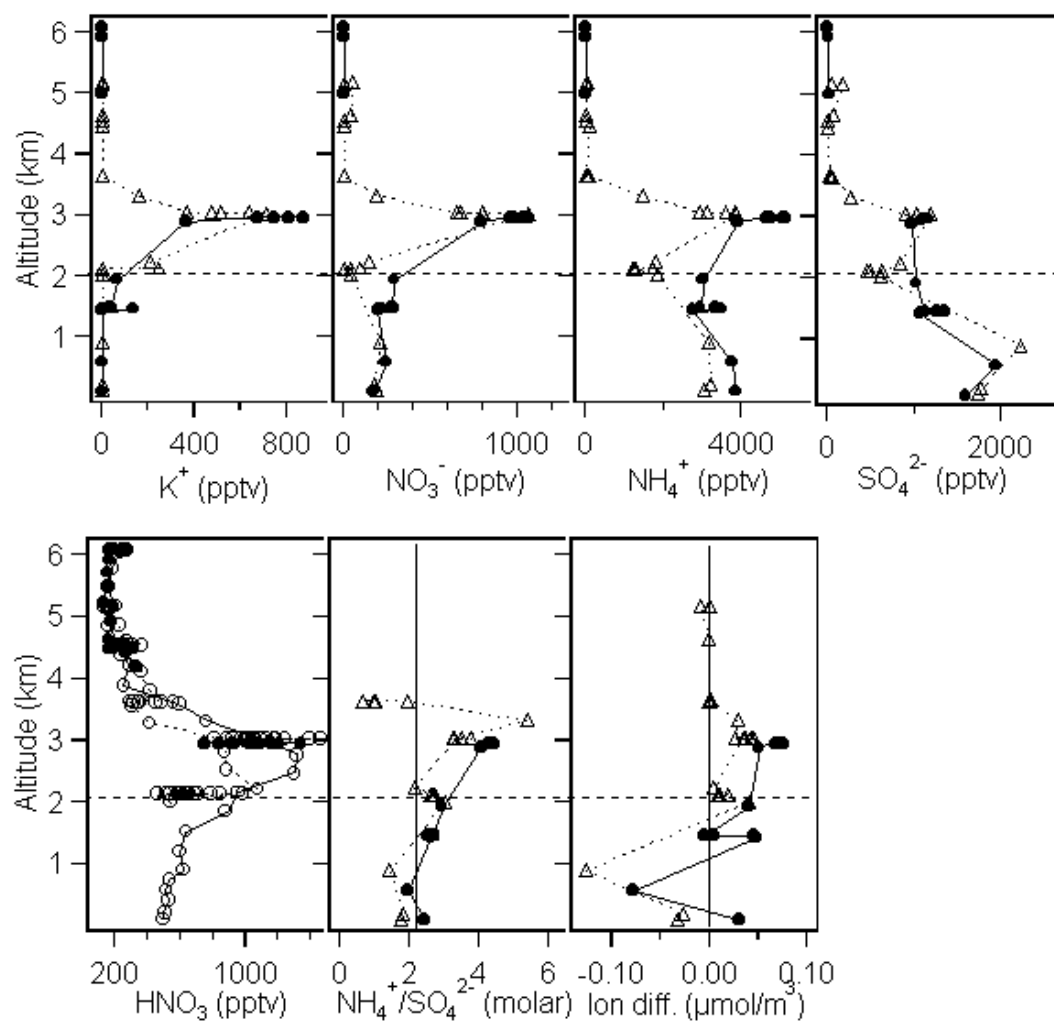


Figure 9.

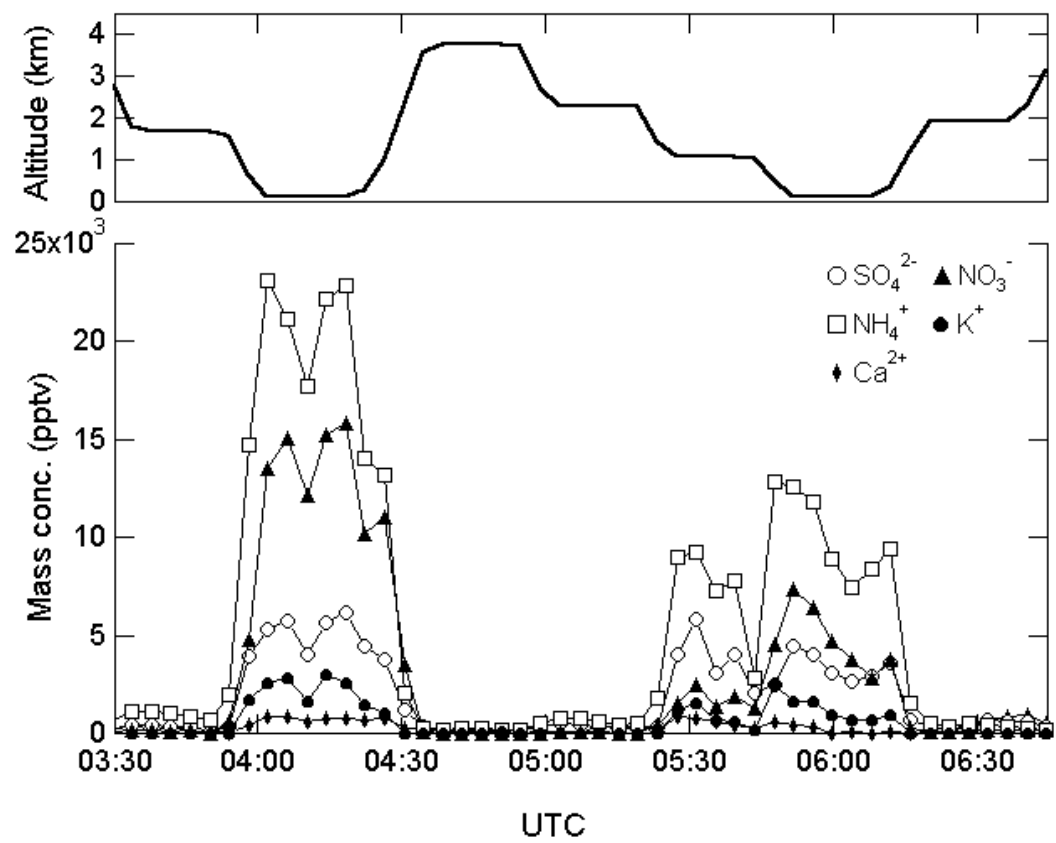


Figure 10

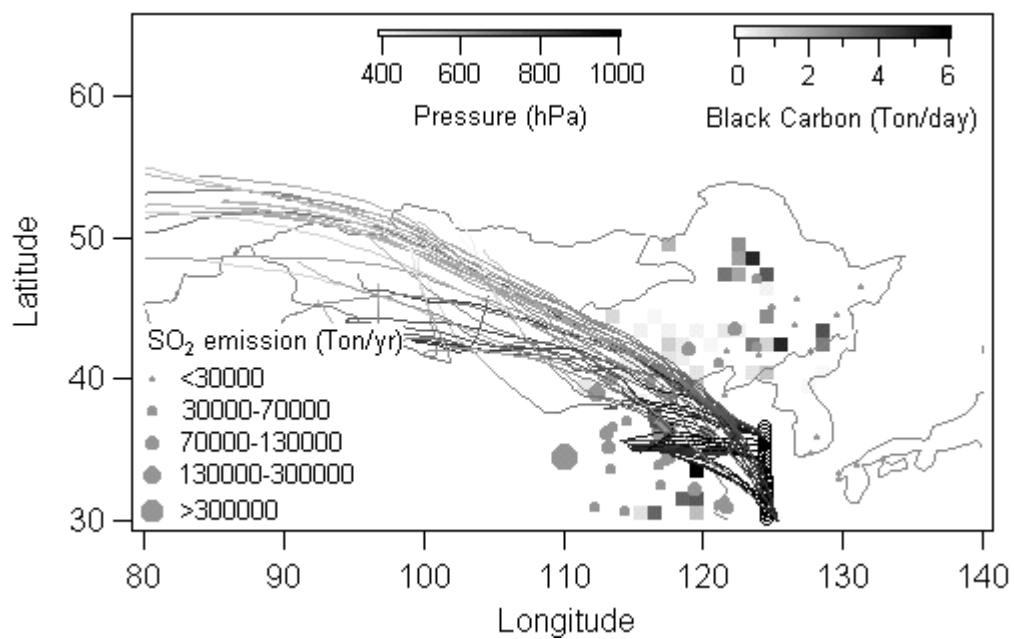
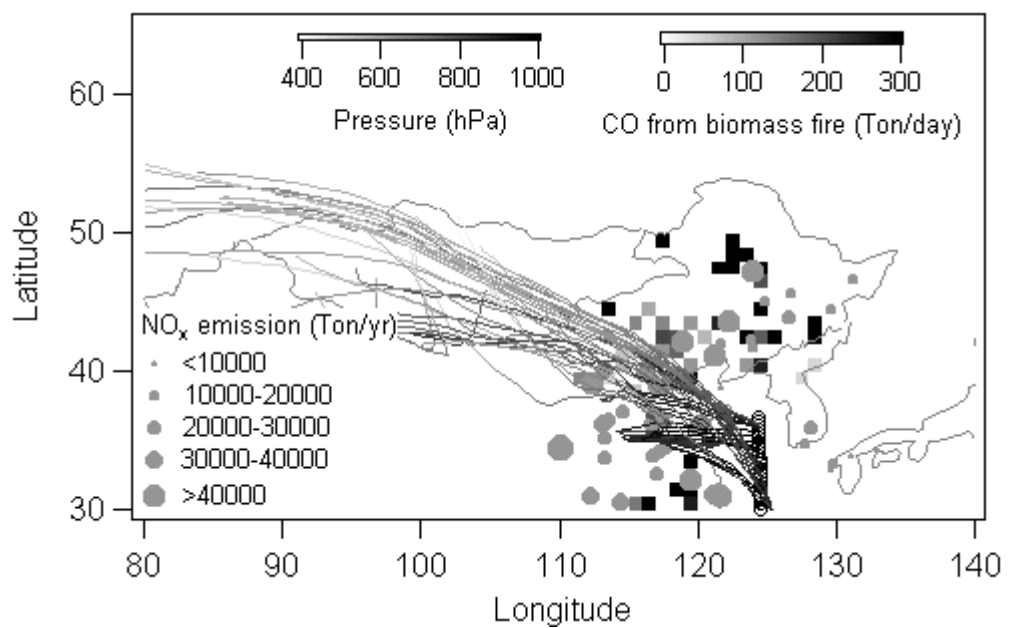


Figure 11

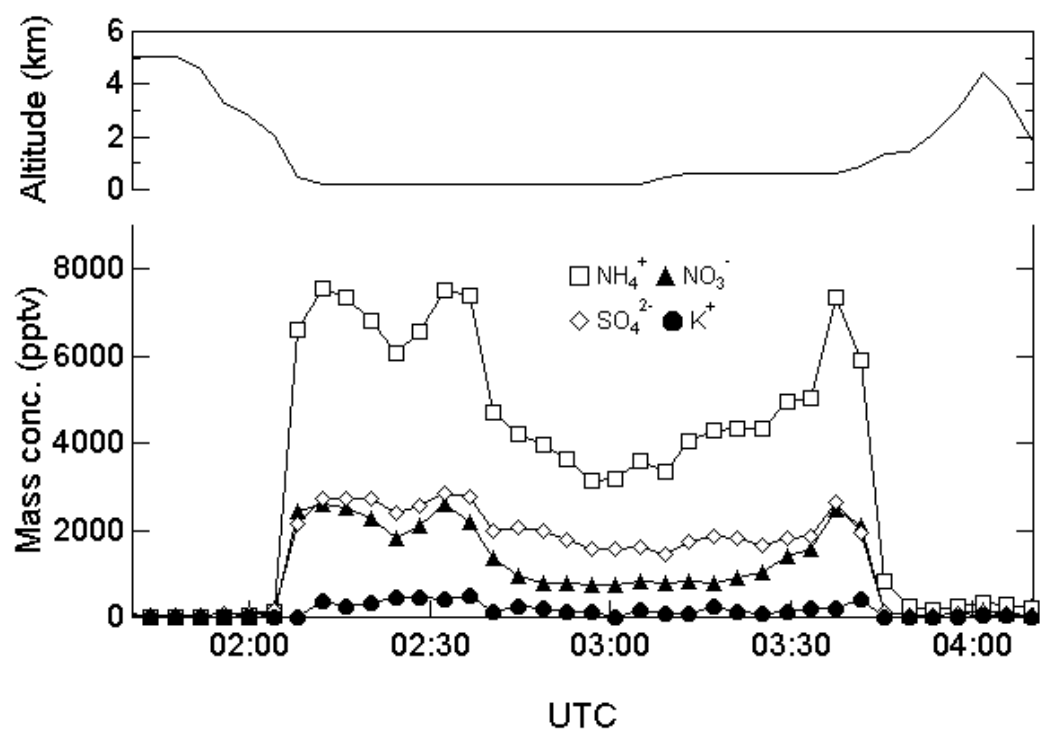


Figure 12

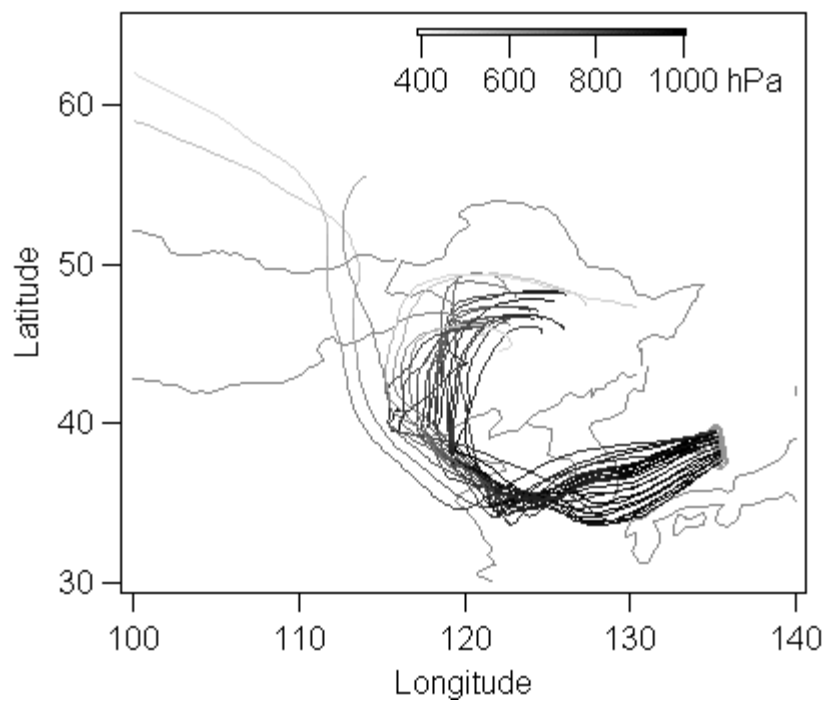


Figure 13

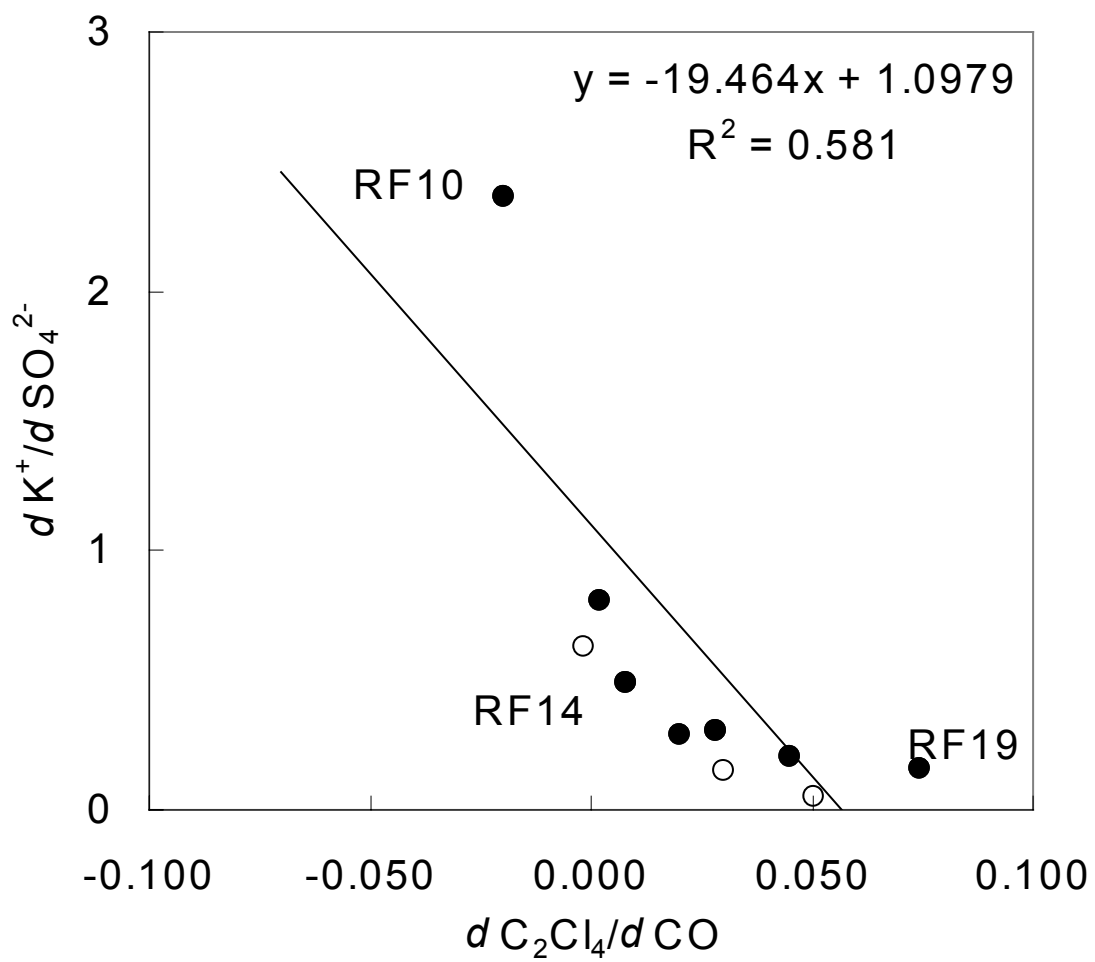


Figure 14

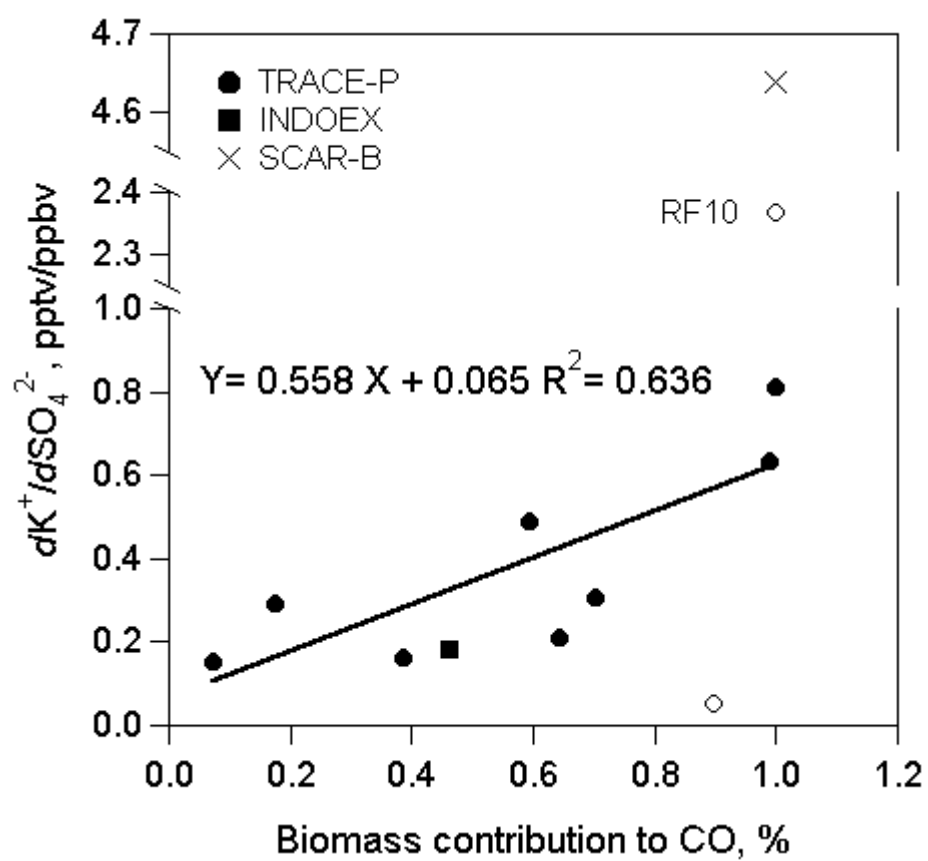


Figure 15

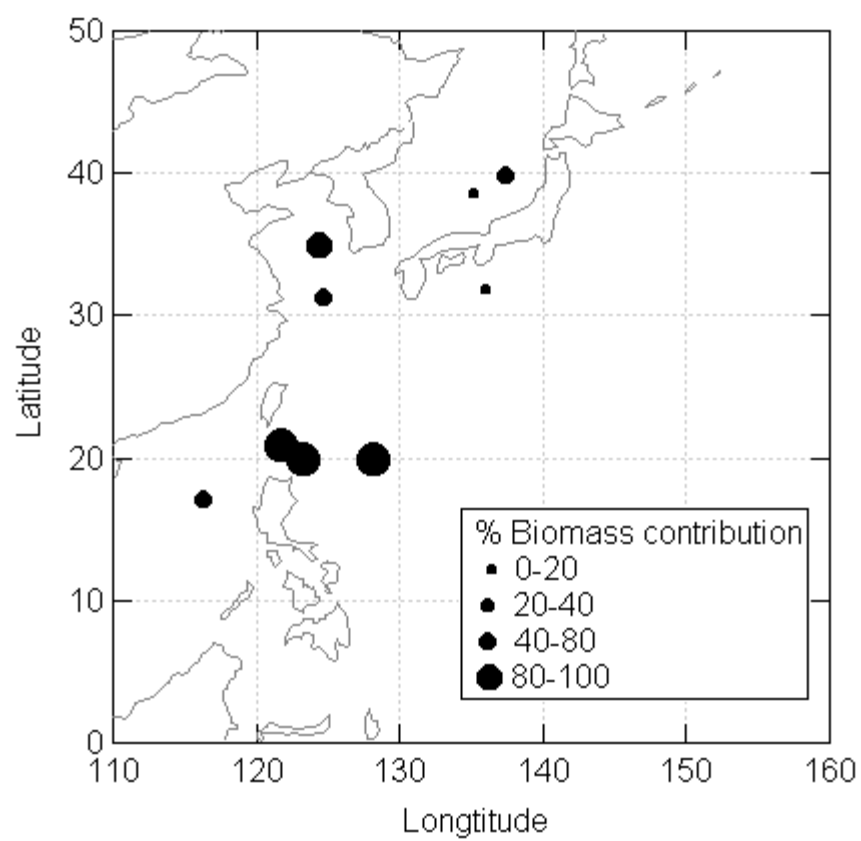


Figure 16